Block Transforms in Progressive Image Coding

Trac D. Tran and Truong Q. Nguyen

1 Introduction

Block transform coding and subband coding have been two dominant techniques in existing image compression standards and implementations. Both methods actually exhibit many similarities: relying on a certain transform to convert the input image to a more decorrelated representation, then utilizing the same basic building blocks such as bit allocator, quantizer, and entropy coder to achieve compression.

Block transform coders enjoyed success first due to their low complexity in implementation and their reasonable performance. The most popular block transform coder leads to the current image compression standard JPEG [1] which utilizes the 8×8 Discrete Cosine Transform (DCT) at its transformation stage. At high bit rates (1 bpp and up), JPEG offers almost visually lossless reconstruction image quality. However, when more compression is needed (i.e., at lower bit rates), annoying blocking artifacts show up because of two reasons: (i) the DCT bases are short, non-overlapped, and have discontinuities at the ends; (ii) JPEG processes each image block independently. So, inter-block correlation has been completely abandoned.

The development of the lapped orthogonal transform [2] and its generalized version GenLOT [3, 4] helps solve the blocking problem to a certain extent by borrowing pixels from the adjacent blocks to produce the transform coefficients of the current block. Lapped transform outperforms DCT on two counts: (i) from the analysis viewpoint, it takes into account inter-block correlation, hence, provides better energy compaction that leads to more efficient entropy coding of the coefficients; (ii) from the synthesis viewpoint, its basis functions decay asymptotically to zero at the ends, reducing blocking discontinuities drastically. However, earlier lapped-transform-based image coders [2, 3, 5] have not utilized global information to their full advantage: the quantization and the entropy coding of transform coefficients are still independent from block to block.

Recently, subband coding has emerged as the leading standardization candidate in future image compression systems thanks to the development of the discrete wavelet transform. Wavelet representation with implicit overlapping and variable-length basis functions produces smoother and more perceptually pleasant reconstructed images. Moreover, wavelet's multiresolution characteristics have created an intuitive foundation on which simple, yet sophisticated, methods of encoding the transform coefficients are developed. Exploiting the relationship between the parent and the offspring coefficients in a wavelet tree, progressive wavelet coders [6, 7, 9] can effectively order the coefficients by bit planes and transmit more significant bits first. This coding scheme results in an embedded bit stream along with many other advantages such as exact bit rate control and near-idempotency

(perfect idempotency is obtained when the transform maps integers to integers). In these subband coders, global information is taken into account fully.

From a frequency domain point of view, the wavelet transform simply provides an octave-band representation of signals. The dyadic wavelet transform is analogous to a non-uniform-band lapped transform. It can sufficiently decorrelate smooth images; however, it has problems with images with well-localized high frequency components, leading to low energy compaction. In this appendix, we shall demonstrate that the embedded framework is not only limited to the wavelet transform; it can be utilized with uniform-band lapped transforms as well. In fact, a judicious choice of appropriately-optimized lapped transform coupled with several levels of wavelet decomposition of the DC band can provide much finer frequency spectrum partitioning, leading to significant improvement over current wavelet coders. This appendix also attempts to shed some light onto a deeper understanding of wavelets, lapped transforms, their relation, and their performance in image compression from a multirate filter bank perspective.

2 The wavelet transform and progressive image transmission

Progressive image transmission is perfect for the recent explosion of the internet. The wavelet-based progressive coding approach first introduced by Shapiro [6] relies on the fundamental idea that more important information (defined here as what decreases a certain distortion measure the most) should be transmitted first. Assume that the distortion measure is the mean-squared error (MSE), the transform is paraunitary, and transform coefficients $c_{i,j}$ are transmitted one by one, it can be proven that the mean squared error decreases by $\frac{|c_{i,j}|}{N}$, where N is the total number of pixels [16]. Therefore, larger coefficients should be transmitted first. If one bit is transmitted at a time, this approach can be generalized to ranking the coefficients by bit planes and the most significant bits are transmitted first [8]. The progressive transmission scheme results in an embedded bit stream (i.e., it can be truncated at any point by the decoder to yield the best corresponding reconstructed image). The algorithm can be thought of as an elegant combination of a scalar quantizer with power-of-two stepsizes and an entropy coder to encode wavelet coefficients.

Embedded algorithm relies on the hierachical coefficients' tree structure that we called a *wavelet tree*, defined as a set of wavelet coefficients from different scales that belong in the same spatial locality as demonstrated in Figure 1(a), where the tree in the vertical direction is circled. All of the coefficients in the lowest frequency band make up the *DC band* or the *reference signal* (located at the upper left corner). Besides these DC coefficients, in a wavelet tree of a particular direction, each lower-frequency *parent node* has four corresponding higher-frequency *offspring nodes*. All coefficients below a parent node in the same spatial locality is defined as its *descendents*. Also, define a coefficient $c_{i,j}$ to be *significant* with respect to a given threshold T if $|c_{i,j}| \geq T$, and *insignificant* otherwise. Meaningful image statistics have shown that if a coefficient is insignificant, it is very likely that its offspring and descendents are insignificant as well. Exploiting this fact, the most sophisticated embedded wavelet coder SPIHT can output a single binary marker

to represent very efficiently a large, smooth image area (an insignificant tree). For more details on the algorithm, the reader is refered to [7].

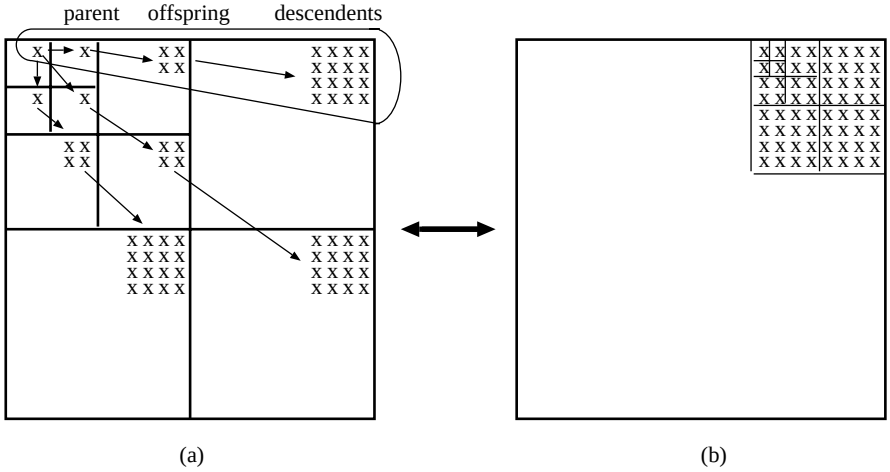

FIGURE 1. Wavelet and block transform analogy.

Although the wavelet tree provides an elegant hierachical data structure which facilitates quantization and entropy coding of the coefficients, the efficiency of the coder still heavily depends on the transform's ability in generating insignificant trees. For non-smooth images that contain a lot of texture, the wavelet transform is not as efficient in signal decorrelation comparing to transforms with finer frequency selectivity and superior energy compaction. Uniform-band lapped transforms hold the edge in this area.

3 Wavelet and block transform analogy

Instead of obtaining an octave-band signal decomposition, one can have a finer uniform-band partitioning as depicted in Figure 2 (drawn for $M = 8$). The finer frequency partitioning compacts more signal energy into a fewer number of coefficients and generates more insignificant ones, leading to an enhancement in the performance of the zerotree algorithm. However, uniform filter bank also has uniform downsampling (all subbands now have the same size). A parent node does not have four offspring nodes as in the case of the wavelet representation. How would one come up with a new tree structure that still takes full advantage of the inter-scale correlation between block-transform coefficients?

The above question can be answered by investigating an analogy between the wavelet and block transform as illustrated in Figure 1. The parent, the offspring, and the descendents in a wavelet tree cover the same spatial locality, and so are the coefficients of a transform block. In fact, a wavelet tree in an L-level decomposition is analogous to a 2^L-channel transform's coefficient block. The difference lies at the bases that generate these coefficients. It can be shown that a 1D L-level wavelet

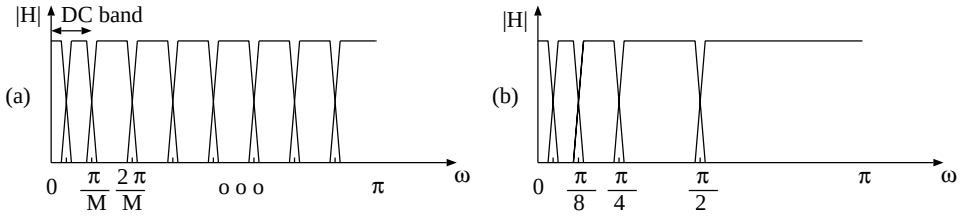

FIGURE 2. Frequency spectrum partitioning of (a) M-channel uniform-band transform (b) dyadic wavelet transform.

decomposition, if implemented as a lapped transform, has the following coefficient matrix:

$$\mathbf{P}_L = \begin{bmatrix} h_0[n] * h_0[\frac{n}{2}] * \cdots * h_0[\frac{n}{2^{L-2}}] * h_0[\frac{n}{2^{L-1}}] \\ h_0[n] * h_0[\frac{n}{2}] * \cdots * h_0[\frac{n}{2^{L-2}}] * h_1[\frac{n}{2^{L-1}}] \\ h_0[n] * h_0[\frac{n}{2}] * \cdots * h_1[\frac{n}{2^{L-2}}] \\ h_0[n] * h_0[\frac{n}{2}] * \cdots * h_1[\frac{n}{2^{L-2}}] \\ \vdots \\ h_1[n] \\ h_1[n] \\ h_1[n] \\ h_1[n] \end{bmatrix}. \tag{1.1}$$

From the coefficient matrix $\mathbf{P}_L$, we can observe several interesting and important characteristics of the wavelet transform through the block transform's prism:

- The wavelet transform can be viewed as a lapped transform with filters of variable lengths. For an L-level decomposition, there are 2^L filters.
- Each basis function has linear phase; however, they do not share the same center of symmetry.
- The block size is defined by the length of the longest filter. If $h_0[n]$ is longer and has length N_0, the longest filter is on top, covering the DC component, and it has a length of $(2^L - 1)(N_0 - 1) + 1$. For the biorthogonal wavelet pair with $h_0[n]$ of length 9 and $h_1[n]$ of length 7 and $L = 3$, the eight resulting basis functions have lengths of $57, 49, 21, 21, 7, 7, 7$, and 7.
- For a 6-level decomposition using the same $9-7$ pair, the length of the longest basis function grows to 505! The huge amount of overlapped pixels explains the smoothness of as well as the complete elimination of blocking artifacts in wavelet-based coders' reconstructed images.

Each block of lapped transform coefficients represents a spatial locality similarly to a tree of wavelet coefficients. Let $\mathcal{O}(i,j)$ be the set of coordinates of all offspring of the node (i,j) in an M-channel block transform ($0 \le i,j \le M-1$), then $\mathcal{O}(i,j)$ can be represented as follows:

$$\mathcal{O}(i,j) = \{(2i,2j),(2i,2j+1),(2i+1,2j),(2i+1,2j+1)\}. \tag{1.2}$$

All $(0,0)$ coefficients from all transform blocks form the DC band, which is similar to the wavelet transform's reference signal, and each of these nodes has only three offsprings: $(0,1)$, $(1,0)$, and $(1,1)$. This is a straightforward generalization of the structure first proposed in [10]. The only requirement here is that the number of channel M has to be a power of two. Figure 3 demonstrates through a simple rearrangement of the block transform coefficients that the redefined tree structure above does possess a wavelet-like multiscale representation. The quadtree grouping of the coefficients is far from optimal in the rate-distortion sense; however, other parent-offspring relationships for uniform-band transform such as the one mentioned in [6] do not facilitate the further usage of various entropy coders to increase the coding efficiency.

FIGURE 3. Demonstration of the analogy between uniform-band transform and wavelet representation.

4 Transform Design

A mere replacement of the wavelet transform by low-complexity block transforms is not enough to compete with SPIHT as testified in [10, 11]. We propose below several novel criteria in designing high-performance lapped transforms. The overall cost used for transform optimization is a combination of coding gain, DC attenuation, attenuation around the mirror frequencies, weighted stopband attenuation, and unequal-length constraint on filter responses:

$$C_{\text{overall}} = \alpha_1 C_{\text{coding gain}} + \alpha_2 C_{\text{DC}} + \alpha_3 C_{\text{mirror}} + \alpha_4 C_{\text{weighted-stopband}} + \alpha_5 C_{\text{unequal-length}}. \tag{1.3}$$

The first three cost functions are well-known criteria for image compression. Among them, higher coding gain correlates most consistently with higher objective performance (PSNR). Transforms with higher coding gain compact more energy into a fewer number of coefficients, and the more significant bits of those coefficients always get transmitted first. All designs in this appendix are obtained with a version of the generalized coding gain formula in [19]. Low DC leakage and high attenuation near the mirror frequencies are not as essential to the coder's objective performance as coding gain. However, they do improve the visual quality of the reconstructed image [5, 17].

The ramp-weighted stopband attenuation cost is defined as

$$C_{\text{weighted-stopband}} = \sum_{k=1}^{M-1} \int_{\omega \in \Omega_S} |W_k(e^{j\omega}) H_k(e^{j\omega})|^2 d\omega,$$

where $W_k(e^{j\omega})$ is a linear function starting with value one at the peak of the frequency response decaying to zero at DC. The frequency weighting forces the highband filters to pick up as little energy as possible, ensuring a high number of insignificant trees. This cost function also helps the optimization process in obtaining higher coding gains.

The unequal-length constraint forces the tails of the high-frequency band-pass filters' responses to have very small values (not necessarily zeroes). The higher the frequency band, the shorter the effective length of the filter gets. This constraint is added to minimize the ringing around strong image edges at low bit rates, a typical characteristic of transforms with long filter lengths. Similar ideas have been presented in [20, 26, 27] where the filters have different lengths. However, these methods restrict the parameter search space severely, leading to low coding gains.

High-performance lapped transforms designed specifically for progressive image coding are presented in Figure 4(c)-(d). Figure 4(a) and (b) show the popular DCT and LOT for comparison purposes. The frequency response and the basis functions of the 8-channel 40-tap GenLOT shown in Figure 4(c) exemplify a well-optimized filter bank: high coding gain and low attenuation near DC for best energy compaction, smoothly decaying impulse responses for blocking artifacts elimination, and unequal-length filters for ringing artifacts suppression.

Figure 3 shows that there still exists correlation between DC coefficients. To decorrelate the DC band even more, several levels of wavelet decomposition can be used depending on the input image size. Besides the obvious increase in the coding efficiency of DC coefficients thanks to a deeper coefficient trees, wavelets provide variably longer bases for the signal's DC component, leading to smoother reconstructed images, i.e., blocking artifacts are further reduced. Regularity objective can be added in the transform design process to produce M-band wavelets, and a wavelet-like iteration can be carried out using uniform-band transforms as well. The complete coder's diagram is depicted in Figure 5.

5 Coding Results

The objective coding results (PSNR in dB) for standard 512×512 Lena and Barbara test images are tabulated in Table 1.1 where several different transforms are used:

- DCT, 8-channel 8-tap filters, shown in Figure 4(a).
- LOT 8-channel 16-tap filters, shown in Figure 4(b).
- GenLOT, 8-channel 40-tap filters, shown in Figure 4(c).
- LOT, 16-channel 32-tap filters, shown in Figure 4(d).

The block transform coders are compared to the best progressive wavelet coder SPIHT [7] and an earlier DCT-based embedded coder [10]. All computed PSNR quotes in dB are obtained from a real compressed bit stream with all overheads included. The rate-distortion curves in Figure 6 and the tabulated coding results

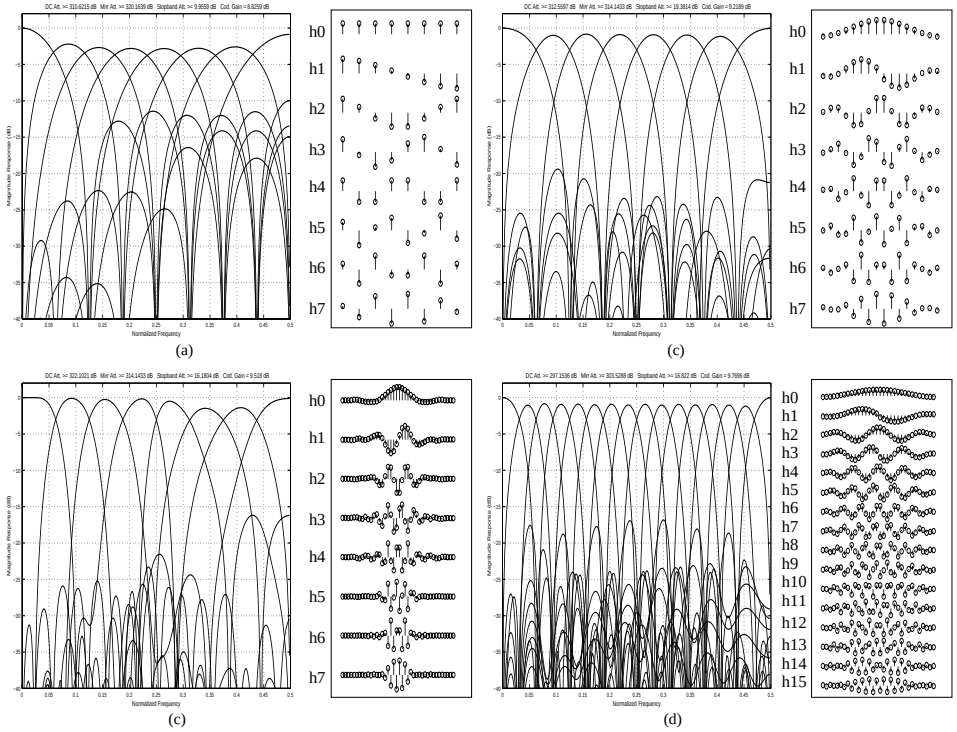

FIGURE 4. Frequency and impulse responses of orthogonal transforms: (a) 8-channel 8-tap DCT (b) 8-channel 16-tap LOT (c) 8-channel 40-tap GenLOT (d) 16-channel 32-tap LOT.

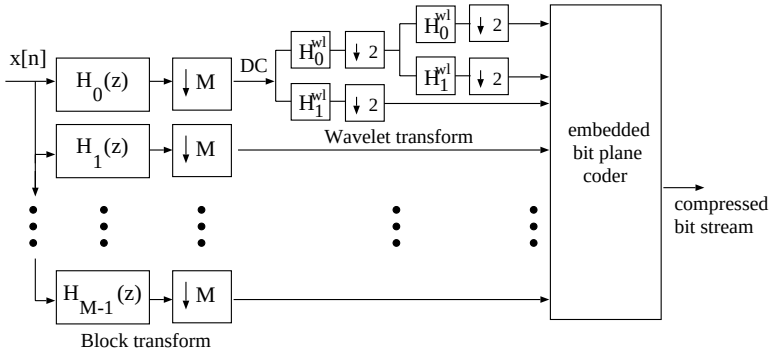

FIGURE 5. Complete coder's diagram.

in Table 1.1 clearly demonstrate the superiority of well-optimized lapped transforms over wavelets. For a smooth image like Lena where the wavelet transform can sufficiently decorrelate, SPIHT offers a comparable performance. However, for a highly-textured image like Barbara, the 8×40 GenLOT and the 16×32 LOT coder can provide a PSNR gain of around 2 dB over a wide range of bit rates.

Lena	Progressive Transmission Coders					
Comp. Ratio	SPIHT (9-7WL)	Xiong et al (DCT)	8 x 8 DCT	8 x 16 LOT	8 x 40 GenLOT	16 x 32 LOT
1:8	40.41	39.62	39.91	40.09	40.43	40.16
1:16	37.21	36.00	36.38	36.75	37.32	36.96
1:32	34.11	32.25	32.90	33.57	34.23	33.87
1:64	31.10	--	29.67	30.48	31.16	30.85
1:100	29.35	--	27.80	28.61	29.31	28.98
1:128	28.38	--	26.91	27.61	28.35	27.99

(a)

Barbara	Progressive Transmission Coders					
Comp. Ratio	SPIHT (9-7WL)	Xiong et al (DCT)	8 x 8 DCT	8 x 16 LOT	8 x 40 GenLOT	16 x 32 GLBT
1:8	36.41	36.10	36.31	37.43	38.08	38.02
1:16	31.40	30.82	31.11	32.70	33.47	33.47
1:32	27.58	26.83	27.28	28.80	29.53	29.70
1:64	24.86	--	24.58	25.70	26.37	26.63
1:100	23.76	--	23.42	24.34	24.95	25.14
1:128	23.35	--	22.68	23.37	24.01	24.09

(b)

TABLE 1.1. Coding results of various progressive coders (a) for Lena (b) for Barbara.

Unlike other block transform coders whose performance dramatically drops at very high compression ratios, the new progressive coders are consistent throughout as illustrated in Figure 6. Lastly, better decorrelation of the DC band provides around $0.3 - 0.5$ dB improvement over the earlier DCT embedded coder in [10].

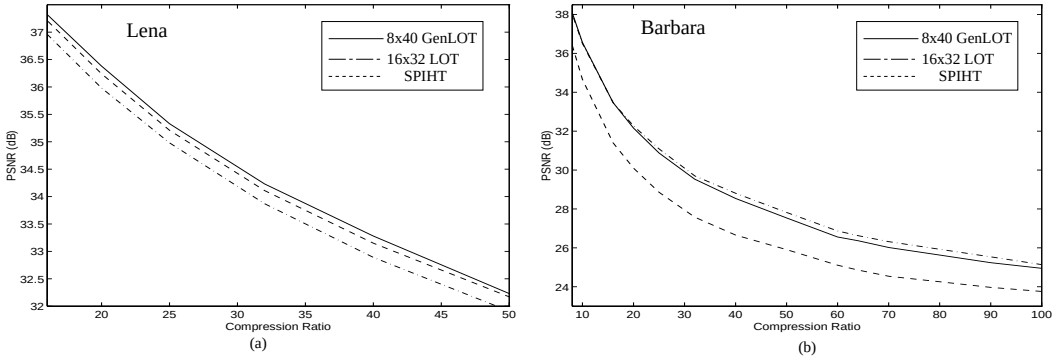

FIGURE 6. Rate-distortion curves of various progressive coders (a) for Lena (b) for Barbara.

Figure 7 - 9 confirm lapped transforms' superiority in reconstructed image quality as well. Figure 7 shows reconstructed Barbara images at 1:32 by various block transforms. Comparing to JPEG, blocking artifacts are already remarkably reduced in the DCT-based coder in Figure 7(a). Blocking is completely eliminated when DCT is replaced by better lapped transforms as shown in Figure 7(c)-(d), and Figure 8. A closer look in Figure 9(a)-(c) (where only 256×256 image portions are shown so that artifacts can be more easily seen) reveals that besides blocking elimination, good lapped transform can preserve texture beautifully (the table cloth and the clothes pattern) while keeping the edges relatively clean. The absence of excessive ringing considering the transform's long filters should not come across as a surprise: a glimpse of the time responses of the GenLOT in Figure 4(c) reveals that the high-frequency bandpasses and the highpass filter are very carefully designed – their lengths are essentially under 16-tap. Comparing to SPIHT, the reconstructed images have an overall sharper and more natural look with more defining edges and more evenly reconstructed texture regions. Although the PSNR difference is not as striking in the Goldhill image, the improvement in perceptual quality is rather sig-

nificant as shown in Figure 9(d)-(f). Even at 1:100, the reconstructed Goldhill image in Figure 8(d) is still visually pleasant: no blocking and not much ringing. More objective and subjective evaluation of block-transform-based progressive coding can be found at *http://saigon.ece.wisc.edu/~waveweb/Coder/index.html*.

FIGURE 7. Barbara coded at 1:32 by (a) 8×8 DCT (b) 8×16 LOT (c) 8×40 GenLOT (d) 16×32 LOT.

As previously mentioned, the improvement over wavelets keys on the lapped transform's ability to capture and separate localized signal components in the frequency domain. In the spatial domain, this corresponds to images with directional repetitive texture patterns. To illustrate this point, the lapped-transform-based

(a) (b)

(c) (d)

FIGURE 8. Goldhill coded by the 8×40 GenLOT coder at (a) 1:16, 33.36 dB (b) 1:32, 30.79 dB (c) 1:64, 28.60 dB (d) 1:100, 27.40 dB.

coder is compared against the FBI Wavelet Scalar Quantization (WSQ) standard [23]. When the original 768×768 gray-scale fingerprint image is shown in Figure 10(a) is compressed at $1 : 13.6$ (43366 bytes) by WSQ, Bradley *et al* reported a PSNR of 36.05 dB. Using the 16×32 LOT in Figure 4(d), a PSNR of 37.87 dB can be achieved at the same compression ratio. For the same PSNR, the LOT coder can compress the image down to $1 : 19$ where the reconstructed image is shown in Figure 10(b). To put this in perspective, the wavelet packet SFQ coder in [22] reported a PSNR of only 37.30 dB at 1:13.6 compression ratio. At $1 : 18.036$ (32702 bytes), WSQ's reconstructed image as shown in Figure 10(c) has a PSNR of 34.42

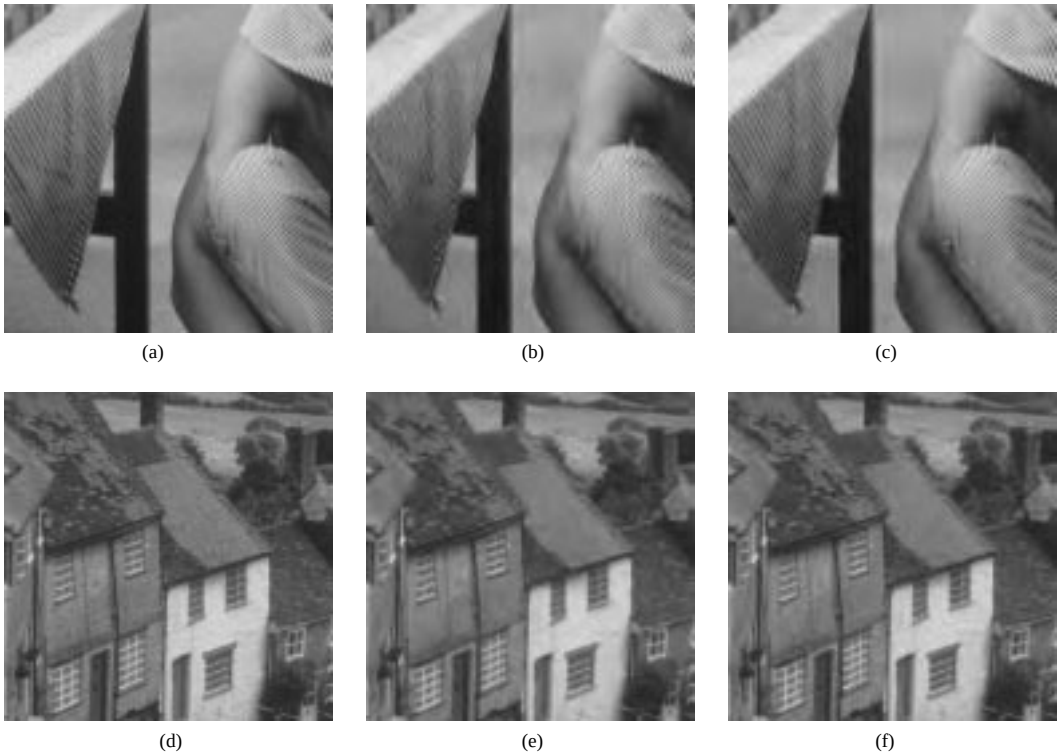

FIGURE 9. Perceptual comparison between wavelet and block transform embedded coder. Zoom-in portion of (a) original Barbara (b) SPIHT at 1:32 (c) 8×40 GenLOT embedded coder at 1:32 (d) original Goldhill (e) SPIHT at 1:32 (c) 8×40 GenLOT embedded coder at 1:32.

dB while the LOT coder produces 36.32 dB. At the same distortion, we can compress the image down to a compression ratio of 1:26 (22685 bytes) as shown in Figure 10(d). Notice the high perceptual image quality in Figure 10(b) and (d): no visually disturbing blocking and ringing artifacts.

6 References

[1] W. B. Pennebaker and J. L. Mitchell, *JPEG: Still Image Compression Standard*, Van Nostrand Reinhold, 1993.

[2] H. S. Malvar, *Signal Processing with Lapped Transforms*, Artech House, 1992.

[3] R. de Queiroz, T. Q. Nguyen, and K. Rao, "The GenLOT: generalized linear-phase lapped orthogonal transform," *IEEE Trans. on SP,* vol. 40, pp. 497-507, Mar. 1996.

[4] T. D. Tran and T. Q. Nguyen, "On M-channel linear-phase FIR filter banks and application in image compression," *IEEE Trans. on SP,* vol. 45, pp. 2175-2187, Sept. 1997.

[5] S. Trautmann and T. Q. Nguyen, "GenLOT – design and application for

(a)

(b)

(c)

(d)

FIGURE 10. (a) original Fingerprint image (589824 bytes) (b) coded by the 16×32 LOT coder at 1:19 (31043 bytes), 36.05 dB (c) coded by WSQ coder at 1:18 (32702 bytes), 34.43 dB (d) coded by the 16×32 LOT coder at 1:26 (22685 bytes), 34.42 dB.

transform-based image coding," *Asilomar conference*, Monterey, Nov. 1995.

[6] J. M. Shapiro, "Embedded image coding using zerotrees of wavelet coefficients," *IEEE Trans. on SP,* vol. 41, pp. 3445-3462, Dec. 1993.

[7] A. Said and W. A. Pearlman, "A new fast and efficient image codec on set partitioning in hierarchical trees," *IEEE Trans on Circuits Syst. Video Tech.,* vol. 6, pp. 243-250, June 1996.

[8] M. Rabbani and P. W. Jones, *Digital Image Compression Techniques,* SPIE Opt. Eng. Press, Bellingham, Washington, 1991.

[9] "Compression with reversible embedded wavelets," RICOH Company Ltd. submission to ISO/IEC JTC1/SC29/WG1 for the JTC1.29.12 work item, 1995. Can be obtained on the World Wide Web, address: *http://www.crc.ricoh.com/CREW*.

[10] Z. Xiong, O. Guleryuz, and M. T. Orchard, "A DCT-based embedded image coder," *IEEE SP Letters*, Nov 1996.

[11] H. S. Malvar, "Lapped biorthogonal transforms for transform coding with reduced blocking and ringing artifacts," *ICASSP*, Munich, April 1997.

[12] T. D. Tran, R. de Queiroz, and T. Q. Nguyen, "The generalized lapped biorthogonal transform," *ICASSP,* Seattle, May 1998.

[13] P. P. Vaidyanathan, *Multirate Systems and Filter Banks*, Prentice Hall, 1993.

[14] G. Strang and T. Q. Nguyen, *Wavelets and Filter Banks*, Wellesley-Cambridge Press, 1996.

[15] M. Vetterli and J. Kovacevic, *Wavelets and Subband Coding*, Prentice-Hall, 1995.

[16] R. A. DeVore, B. Jawerth, and B. J. Lucier, "Image compression through wavelet trasnform coding," *IEEE Trans on Information Theory*, vol. 38, pp. 719-746, March, 1992.

[17] T. A. Ramstad, S. O. Aase, J. H. Husoy, *Subband Compression of Images: Principles and Examples*, Elsevier, 1995.

[18] A. Soman, P. P. Vaidyanathan, and T. Q. Nguyen, "Linear phase paraunitary filter banks," *IEEE Trans. on SP,* V. 41, pp. 3480-3496, 1993.

[19] J. Katto and Y. Yasuda, "Performance evaluation of subband coding and optimization of its filter coefficients," *SPIE Proc. Visual Comm. and Image Proc.*, 1991.

[20] T. D. Tran and T. Q. Nguyen, "Generalized lapped orthogonal transform with unequal-length basis functions," *ISCAS*, Hong Kong, June 1997.

[21] Z. Xiong, K. Ramchandran, and M. T. Orchard, "Space-frequency quantization for wavelet Image Coding," *IEEE Trans. on Image Processing*, vol. 6, pp. 677-693, May 1997.

[22] Z. Xiong, K. Ramchandran, and M. T. Orchard, "Wavelet packet image coding using space-frequency quantization," *submitted to IEEE Trans. on Image Processing*, 1997.

[23] J. N. Bradley, C. M. Brislawn, and T. Hopper, "The FBI wavelet/scalar quantization standard for gray-scale fingerprint Image Compression," *Proc. VCIP*, Orlando, FL, April 1993.

[24] R.L. Joshi, H. Jafarkhani, J.H. Kasner, T.R. Fischer, N. Farvardin, M.W. Marcellin, and R. H. Bamberger, "Comparison of different methods of classification in subband coding of images," submitted to *IEEE Trans. Image Processing,* 1996.

[25] S.M. LoPresto, K. Ramchandran, and M.T. Orchard, "Image coding based on mixture modeling of wavelet coefficients and a fast estimation-quantization framework," *IEEE DCC Proceedings,* pp. 221-230, March 1997.

[26] M. Ikehara, T. D. Tran, and T. Q. Nguyen, "Linear phase paraunitary filter banks with unequal-length filters," *ICIP,* Santa Barbara, Oct. 1997.

[27] T. D. Tran, M. Ikehara, and T. Q. Nguyen, "Linear phase paraunitary filter bank with variable-length Filters and its Application in Image Compression," submitted to *IEEE Trans. on Signal Processing* in Dec. 1997.